Scanning Mutagenesis Identifies Amino Acid Residues Essential for the *in Vivo* Activity of the *Escherichia coli* DnaJ (Hsp40) J-Domain

Pierre Genevaux,[1] Françoise Schwager, Costa Georgopoulos and William L. Kelley[2]

Département de Biochimie Médicale, Centre Médical Universitaire, CH-1211 Geneva 4, Switzerland

Manuscript received June 16, 2002
Accepted for publication August 9, 2002

ABSTRACT

The DnaJ (Hsp40) cochaperone regulates the DnaK (Hsp70) chaperone by accelerating ATP hydrolysis in a cycle closely linked to substrate binding and release. The J-domain, the signature motif of the Hsp40 family, orchestrates interaction with the DnaK ATPase domain. We studied the J-domain by creating 42 mutant *E. coli* DnaJ variants and examining their phenotypes in various separate *in vivo* assays, namely, bacterial growth at low and high temperatures, motility, and propagation of bacteriophage λ. Most mutants studied behaved like wild type in all assays. In addition to the $_{33}$HisProAsp$_{35}$ (HPD) tripeptide found in all known functional J-domains, our study uncovered three new single substitution mutations (Y25A, K26A, and F47A) that totally abolish J-domain function. Furthermore, two glycine substitution mutants in an exposed flexible loop (R36G, N37G) showed partial loss of J-domain function alone and complete loss of function as a triple (RNQ-GGG) mutant coupled with the phenotypically silent Q38G. Interestingly, all the essential residues map to a small region on the same solvent-exposed face of the J-domain. Engineered mutations in the corresponding residues of the human Hdj1 J-domain grafted in *E. coli* DnaJ also resulted in loss of function, suggesting an evolutionarily conserved interaction surface. We propose that these clustered residues impart critical sequence determinants necessary for J-domain catalytic activity and reversible contact interface with the DnaK ATPase domain.

THE Hsp70 chaperone machine performs many diverse roles in the cell, including folding of nascent proteins, translocation of polypeptides across organelle membranes, coordinating responses to stress, and targeting selected proteins for degradation (Hartl 1996; Bukau and Horwich 1998). Hsp70 chaperone machines can participate in more specialized roles, such as signaling and vesicle trafficking, and such activities have been exploited by viruses, such as influenza, SV40, and bacteriophage λ (Sullivan *et al.* 2000). Mechanistically, the Hsp70 chaperone couples ATP hydrolysis in its N-terminal domain to substrate binding and release in its C-terminal domain. The Hsp40 cochaperones specifically help stimulate ATP hydrolysis and deliver substrates to Hsp70, while other factors, such as GrpE and Bag1, participate in nucleotide exchange (Hartl 1996; Gassler *et al.* 2001).

The J-domain represents an ~70-amino-acid-long residue signature sequence of the Hsp40 family and helps direct specific interaction with the Hsp70 ATPase domain (Liberek *et al.* 1991; Wall *et al.* 1994; Karzai and Mcmacken 1996; Lyman and Schekman 1997; Gassler *et al.* 1998; Greene *et al.* 1998; Kelley 1998; Misselwitz *et al.* 1998; Suh *et al.* 1998). Multiple alignments of various J-domains show significant overall amino acid sequence conservation among evolutionarily diverse organisms (Hennessy *et al.* 2000). High-resolution NMR showed that the J-domain of the *Escherichia coli* DnaJ protein represents a novel fold, composed of two antiparallel coiled coil helices flanking a flexibly disordered solvent-exposed loop that contains the highly conserved His-Pro-Asp (HPD) tripeptide (Szyperski *et al.* 1994; Hill *et al.* 1995; Pellacchia *et al.* 1996; Huang *et al.* 1999). The structures of the J-domains of the human Hdj1 (Qian *et al.* 1996), the polyomavirus T antigen (Berjanskii *et al.* 2000), and the SV40 T antigen in complex with the retinoblastoma tumor-suppressor pocket domain (Kim *et al.* 2001) show a similar overall domain fold, implying an evolutionarily conserved mechanism of Hsp40-Hsp70 interaction. Amino acid substitutions in the HPD tripeptide in the *E. coli* DnaJ, as well as in other Hsp40 J-domains, abolish stimulation of their cognate Hsp70 partner ATPase activity (Wall *et al.* 1994; Tsai and Douglas 1996) and result in loss of function *in vivo*.

In this study, we sought to identify amino acid side chains that comprise the regulatory DnaK/DnaJ contact interface. Alanine and glycine scanning mutants across the entire J-domain coding sequence in *E. coli* DnaJ were engineered, and their mutant phenotypes were analyzed *in vivo* using several independent assays for functional DnaJ cochaperone activity, namely, bacterial growth at low and high temperature (Wall *et al.* 1994; Ueguchi *et al.* 1995), motility (Shi *et al.* 1992), and bacteriophage

[1]*Corresponding author:* Département de Biochimie Médicale, Centre Médical Universitaire, 1, rue Michel-Servet, CH-1211 Genève 4, Switzerland. E-mail: pierre.genevaux@medecine.unige.ch

[2]*Present address:* Division des Maladies Infectieuses, Hôpital Cantonal de Genève, CH-1211 Geneva 14, Switzerland.

λ growth. This genetic approach has allowed the characterization of novel amino acid residues critical for J-domain biological function.

MATERIALS AND METHODS

Bacterial strains and plasmids: *E. coli* WKG190 is MC4100 *dnaJ*::Tn*10*-42 Δ*cbpA*::*kan* and has been described previously (Kelley and Georgopoulos 1997). MG1655 *dnaJ*::Tn*10* Δ*cbpA*::*kan* was constructed by standard bacteriophage P1 transduction. Plasmids pWKG90 and pWKG90H71T have been described (Kelley and Georgopoulos 1997). A 210-bp fragment encoding the J-domain of Hdj1 (Raabe and Manley 1991) was amplified from human genomic DNA (Stratagene, La Jolla, CA) by the polymerase chain reaction (PCR) using the primers 5′-cggaattccatgggtaaagactactaccagacgttg-3′ and 5′-ccggtaccttectccccgtagcggtcgaagatctc-3′, which introduced the appropriate *Eco*RI and *Kpn*I sites (underlined). The fragment was digested with *Eco*RI and *Kpn*I and cloned into plasmid pWKG90H71T digested with the same enzymes to yield pGP18. All DNA manipulations were performed with DH5α or DH10B (Invitrogen/Life Technologies).

Mutagenesis: To be consistent with the DnaJ numbering in the Protein Database (PDB) accession 1XBL (Pellacchia *et al.* 1996), the initiating methionine codon is taken as 1. The *dnaJ* mutants were constructed by two-step PCR site-directed mutagenesis (Higuchi *et al.* 1988), by Quickchange (Stratagene), or by primer extension (Kunkel *et al.* 1987) using plasmid pWKG90 as template. The deletion mutant *dnaJ* ΔhelixIV was constructed using the primer L57 + *Kpn* 5′-ccggtaccagaacttcataagcttc-3′ (*Kpn*I site underlined) and the upstream fusion PCR primer followed by *Eco*RI-*Kpn*I digestion and subcloning into pWKG90H71T cleaved with the same enzymes. The numbering for all *hdj1* mutants uses methionine start codon as 0, consistent with PDB accession 1HDJ (Qian *et al.* 1996). Hdj1 J-domain mutants were constructed in the chimeric plasmid pGP18, using the same two-step PCR-directed mutagenesis strategy. All PCR reactions were performed using *Pfu* polymerase (Stratagene), and the constructs were sequence verified using the appropriate primers.

Immunoblot analysis: Whole-cell extracts were prepared as previously described (Kelley and Georgopoulos 1997). For steady-state protein analysis, DnaJ proteins were resolved in 12% (w/v) polyacrylamide SDS gels stained with Coomassie blue or transferred to polyvinylidene difluoride membranes (Bio-Rad, Hercules, CA), probed with polyclonal rabbit anti-DnaJ antibody, and developed with goat anti-rabbit IgG/horseradish peroxidase-conjugated secondary antibody and enhanced chemiluminescence (Amersham, Buckinghamshire, UK).

***In vivo* DnaJ activity assays:** Bacteriophage λ*d*I (clear plaque former) and λ*d*I *dnaJ*$^{+}$ transducing plaque-forming assays were performed at 30° as described (Kelley and Georgopoulos 1997). For bacterial viability assays, fresh single-colony plasmid transformants in WKG90 were grown overnight at 30° and serially diluted, and aliquots were spotted on Luria-Bertani (LB) agar plates supplemented with 50 μg/ml ampicillin, with or without L-arabinose. Plates were incubated at 30° and 40° for 20 hr and at 14° for 5 days. Bacterial motility was assessed using fresh single-colony plasmid transformants in MG1655 Δ*cbpA dnaJ*-Tn*10-42* grown to OD_{600} 1.2 in LB broth at 30°. Aliquots (1 μl) were spotted on soft agar plates (1% tryptone, 0.5% NaCl, 0.35% agar), with or without L-arabinose inducer. Motility was analyzed after 6 hr of incubation at 30°. The pBAD22 vector alone and pWKG91 encoding the *dnaJ259* (H33Q) inactivating mutation (Wall *et al.* 1994; Kelley and Georgopoulos 1997) were used as negative controls in all assays.

RESULTS

Choice of mutations for structure and function analysis: The high-resolution structure of the J-domain fold shows that it is stabilized by a core of buried, or partially buried, hydrophobic residues (Szyperski *et al.* 1994; Hill *et al.* 1995; Pellacchia *et al.* 1996). Several key core amino acids exhibit multiple long-range interhelical nuclear Overhauser (NOE) connectivities indicating that their alteration could significantly destabilize the protein, leading to unpredictable phenotypes (Szyperski *et al.* 1994). Thus, in our study, we avoided mutations altering any of the amino acids whose side chains comprise the buried core interface of helices I, II, and III. We instead focused our mutational analysis on those solvent-exposed residues that could comprise the J-domain interaction surface with DnaK. Figure 1 depicts schematically the entire collection of amino acid substitutions and deletions analyzed.

Double and triple mutants rapidly exclude nonessential regions: We first constructed a series of adjacent double- or triple-alanine scanning mutants bounded by amino acid residues 2–55 of the minimal J-domain fold to identify rapidly those regions containing important amino acids. The mutations KQD(3-5)AAA, KT(14-15)AA, RE(19-20)AA, MK(30-31)AA, GD(39-40)AA, KE(41-42)AA, KE(48-49)AA, and KE(51-52)AA did not show any discernible effect upon J-domain function in all assays employed (data not shown). Similarly, single-point mutants E8A, S13A, Y32A, E44A, K46A, Y54A, and E55A showed no effect on J-domain function in any of the assays (data not shown).

We observed that mutation EE(17-18)AA measurably affected J-domain function for bacterial growth only at high temperatures, albeit significantly less than the canonical H33Q inactivating mutation, which totally abolishes all J-domain function (Wall *et al.* 1994; data not shown). The EE(17-18)AA mutation conferred normal motility and sensitivity to bacteriophage λ. When we engineered the separate E17A and E18A point mutations we found that neither single mutation had a discernible phenotype in any assay. E17A and E18A proteins were stable and were produced to levels equivalent to those of wild-type DnaJ (data not shown). In contrast, the EE(17,18)AA double-mutant protein was not detectable either in Coomassie-blue-stained gels or by immunoblot. Most likely, this double amino acid substitution severely disrupts protein stability since residue E17 or E18 acts structurally as the helix II N-cap (Pellacchia *et al.* 1996).

Mutations in the flexible helices II-III loop reveal the importance of the $_{33}$HPDRN$_{37}$ pentapeptide loop: The HPD tripeptide motif, located in the loop joining helices II and III, is highly conserved in all known functional Hsp40 proteins and has been predicted to mediate interaction with DnaK (Wild *et al.* 1992; Szyperski *et al.* 1994). Besides H33Q (*dnaJ*259) and D35N (*dnaJ*236),

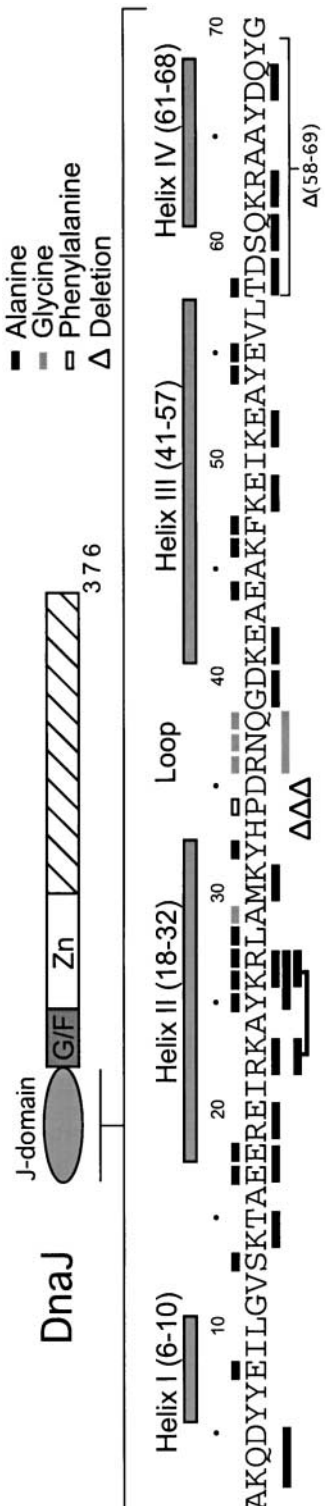

Figure 1.—Summary of the DnaJ J-domain mutants. Other domains of DnaJ are shown as G/F, glycine-phenylalanine rich; Zn, zinc-finger domain; and crosshatching, a less-conserved C-terminal domain. The α-helical boundaries are depicted. The mutation type is indicated by rectangles above (point mutations) or below (multiple) the sequence. The hydrophobic core that stabilizes the J-domain structure is composed principally of buried side chains of residues I9, L10, V12, I21, A53, L57 and also Y25, Y54, Y6, Y7, V56, A24, A29, A54 that are peripherally associated with the core.

no other mutations with significant phenotypes in the *E. coli* DnaJ J-domain have been described (Wall *et al.* 1994; Suh *et al.* 1998). We therefore first designed alanine scanning, deletion, and glycine substitution mutants in residues 33–40 surrounding HPD and comprising the loop. Since the J-domain structure shows the helices II and III loop to be highly disordered (Pellacchia *et al.* 1996; Suh *et al.* 1998), we chose to alter residues 36–38 to glycine to preserve maximal conformational dihedral space. The results of this study are shown in Table 1.

We found that the deletion of H33, P34, or D35 abolished bacterial growth at high and low temperature, although the steady-state mutant protein levels of all mutants were comparable to those of wild type. Motility and bacteriophage λ growth were also concomitantly abolished by these mutations (data not shown). Similarly, the P34F point mutation, which is known to inactivate the SV40 J-domain (Peden and Pipas 1992), abolished DnaJ function in all assays, despite comparable wild-type steady-state protein levels (Table 1; data not shown). Collectively, these results indicate that each of the contiguous highly conserved HPD residues are essential for function in DnaJ.

The triple glycine substitution mutant, RNQ(36-38)GGG, adjacent to the HPD tripeptide, was defective for J-domain function in all assays, although it showed steady-state protein levels comparable to those of wild-type control. Single glycine substitution of each residue R36, N37, and Q38, within the helices II and III loop, revealed that R36 and N37 were also important for J-domain function, while Q38G behaved phenotypically like wild-type DnaJ. Titration of arabinose inducer levels showed that R36G and N37G could not complement for bacterial growth at 0.01% arabinose, whereas at 0.1% arabinose, both mutants could support bacterial growth at low and high temperatures, although the complementation by R36G was reproducibly less robust than that by N37Q (Table 1). The cluster of contiguous critical residues $_{33}$HPDRN$_{37}$ is noteworthy since mutation of residues 38–40 (QGD) following this pentapeptide had no measurable phenotypic effect (Table 1). We conclude that the $_{33}$HPDRN$_{37}$ pentapeptide constitutes an essential region for J-domain function.

F47, in close proximity to H33, is essential for J-domain function: The classical mutation H33Q, or the equivalent change in at least eight other Hsp40 proteins, from organisms including yeast and humans, abolishes J-domain biological function (Wild *et al.* 1992; Wall *et al.* 1994; Tsai and Douglas 1996; Kelley and Georgopoulos 1997). Since the H33 residue is essential, we next examined closely the phenotypes of substitutions of amino acids whose side chains are in close spatial proximity to H33. The side chains of A29, M30, K31, Y32, E44, and F47 are all in close proximity to H33, on the same face of the J-domain (Szyperski *et al.* 1994).

TABLE 1

***In vivo* complementation for growth of strain WKG190 by *dnaJ* carrying mutations in the J-domain**

	No arabinose[a]			0.01% arabinose			0.1% arabinose		
dnaJ	14°	30°	40°	14°	30°	40°	14°	30°	40°
None (vector)	−	+	−	−	+	−	−	+	−
Wild type	−	+	−	+	+	+	+	+	+
H33Q	−	+	−	−	+	−	−	+	−
ΔH33	−	+	−	−	+	−	−	+	−
ΔP34	−	+	−	−	+	−	−	+	−
P34F	−	+	−	−	+	−	−	+	−
ΔD35	−	+	−	−	+	−	−	+	−
RNQ(36-38)GGG	−	+	−	−	+	−	−	+	−
R36G	−	+	−	−	+	−	±	+	±
N37G	−	+	−	−	+	−	+	+	+
Q38G	−	+	−	+	+	+	+	+	+
GD(39-40)AA	−	+	−	+	+	+	+	+	+

+, growth identical to wild type; ±, slow growth; −, no growth at an efficiency of $<10^{-5}$.
[a] Bacterial growth was measured as described in MATERIALS AND METHODS.

We observed that the point mutation F47A, in an amino acid that is partially exposed and that makes no detectable long-range interhelical NOE contacts with other residues (SZYPERSKI *et al.* 1994), abolished all J-domain activity in every assay (Figure 2). In contrast, mutations A29G, MK(30,31)AA, Y32A, and E44A were phenotypically indistinguishable from wild-type DnaJ in each assay (data not shown). Steady-state protein expression levels of mutants were comparable to those of wild-type DnaJ (Figure 2; data not shown). We conclude from this analysis that F47 in αIII is an essential residue for J-domain function.

In this respect, it is important to emphasize that we observed no other alteration of residues in αIII, apart from F47, that resulted in measurable disruption of J-domain function. For example, mutations KE(41,42)AA, E44A, K46A, KE(48,49)AA, KE(51,52)AA, Y54A, and E55A were all phenotypically silent in each assay (data not shown).

Helix II mutations reveal the importance of Y25 and K26: Helix II is amphipathic with a solvent-exposed face composed of predominantly positively charged side chains, evolutionarily conserved among J-domains (HENNESSY *et al.* 2000). We observed that mutations RE(19,20)AA, L28A, and A29G within the helix II boundaries had no significant effect on J-domain activity in any of our *in vivo* assays (data not shown). We next examined seven alanine scanning mutants in the positively charged region encompassing residues 21–27, including a quadruple alanine scanning mutant that replaced all four charged side chains. The results of this study are shown in Figure 3.

We observed that the quadruple mutant RK(22,23)AA/KR(26,27)AA abolished J-domain activity in every assay. Expression of the triple-alanine mutant YKR(25-27)AAA was highly toxic in WGK190 cells and was not investigated further. The double-alanine mutant RK(22,23)AA alone did not show a measurable defect in any assay and could not be distinguished from control cells expressing wild-type DnaJ. In contrast, the double-mutant KR(26,27)AA alone abolished J-domain activity to an extent comparable to the quadruple mutant. These results suggested that the region spanning residues 25–27, but not residues 21–23, was important for J-domain function. To refine this analysis, we next analyzed the phenotypes of the single-alanine mutants Y25A, K26A, and R27A.

As shown in Figure 3, mutant R27A was phenotypically indistinguishable from control wild-type DnaJ, whereas either Y25A or K26A abolished bacterial growth at both low and high temperatures. The phenotype of Y25A was judged more severe since we observed concomitant loss of motility and bacteriophage λ growth, whereas K26A retained partial activity in both the motility and λ plaque assays. Importantly, we observed that K26A acted synergistically with the phenotypically silent R27A mutant, resulting in a double mutant with a more severe phenotype than that of either single-mutant clone. This result suggested that the presence of positively charged side chains at position 26–27 was important for DnaJ function. Consistent with this conclusion, a charge reversal mutant, K26E, showed a more severe inactivating phenotype than that of K26A in all assays employed (data not shown). Control immunoblots showed that the steady-state levels of all mutant proteins were equivalent to those of wild-type DnaJ (Figure 3). We conclude from this analysis that the solvent-exposed K26 side chain and the partially exposed Y25 side chain in αII are especially important for J-domain function. Taken together, our results reveal a striking demarcation of the contiguous essential loop residues $_{33}$HPDRN$_{37}$, since we observed no measurable phenotypic changes arising with mutants

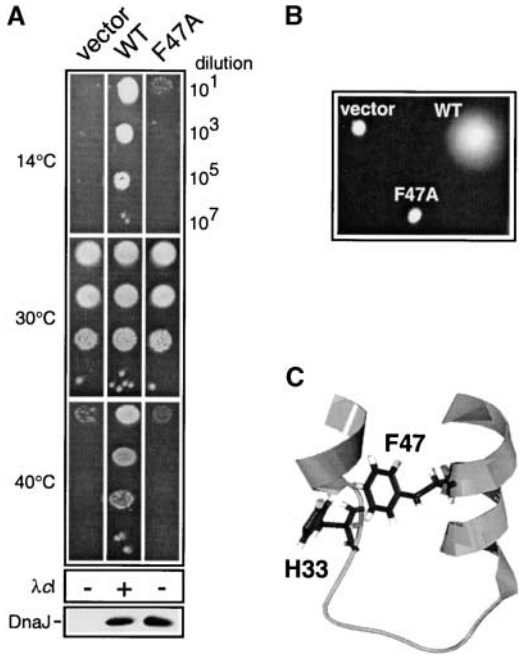

FIGURE 2.—Analysis of DnaJ J-domain mutant phenotypes *in vivo*. (A) Growth temperatures and the fold dilution are indicated. Bacteriophage λ*cI* plaque-forming ability is indicated by + if equivalent to wild-type bacteria or − if $<10^{-5}$ compared to λ*dnaJ*$^+$ transducing bacteriophage control. An immunoblot analysis of whole-cell extracts showing the steady-state expression levels of the wild-type and the mutant DnaJ proteins is presented. (B) Representative bacterial motility assay showing the radial growth of MG1655 *dnaJ*::Tn*10* Δ*cbpA*::*kan* cells containing pWKG90 (WT) compared to those cells containing vector alone or the DnaJ J-domain mutant (F47A). (C) Ribbon diagram showing the close spatial proximity of the F47 aromatic side chain to H33. The figure was generated using PDB coordinates 1XBL (PELLACCHIA *et al.* 1996) and Swiss PdbViewer (http://www.expasy.ch/sbpdv/) and then was rendered with POV-RAY (http://www.povray.org).

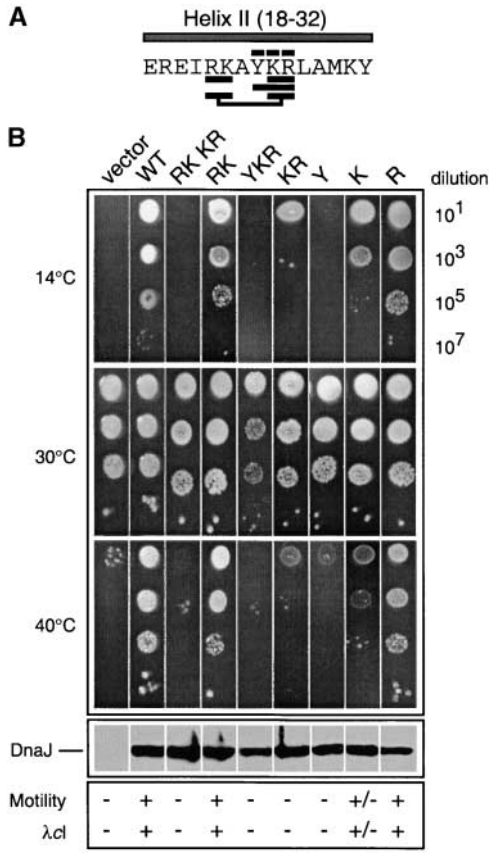

FIGURE 3.—Analysis of J-domain mutant phenotypes in the positively charged region of helix II. (A) The position of mutants is indicated by rectangles as single (above) or multiple mutants (below). (B) Assays were performed as described in the legend to Figure 2A. Motility is indicated by + if cells were comparable to wild-type control and by − if no significant difference from vector control was observed.

in any of the six residues, $_{27}$KLAMKY$_{32}$, preceding, or the four residues, $_{38}$GDKE$_{41}$, following the $_{33}$HPDRN$_{37}$ pentapeptide.

Mutations of helix IV residues exert no measurable effect on J-domain function: A fourth helix, helix IV, terminates the J-domain motif, but its structural role in anchoring the essential fold is minimal (SZYPERSKI *et al.* 1994; PELLACCHIA *et al.* 1996). To examine the role of the helices III and IV loop and of the helix IV residues outside the central 2-55 J-domain fold, we engineered five mutations: T58A, TD(58-59)AA, SQ(60-61)AA, KR(62-63)AA, and DQ(66-67)AA (see Figure 4). We observed that all five alanine scanning mutants behaved phenotypically as wild-type DnaJ in each assay. The steady-state levels of the mutant proteins were also comparable to the levels of wild-type DnaJ (data not shown). We also constructed a complete in-frame deletion of residues 58–69 (inclusive) that eliminated the short interhelical loop and all of helix IV from the *dnaJ* coding sequence. The resulting mutant, DnaJ Δ(58-69), also showed no significant phenotypic difference from wild-type DnaJ in any of our *in vivo* assays under our standard laboratory conditions (Figure 4).

Hdj1 inactivating mutations at the corresponding position of critical DnaJ residues: The overall J-domain fold of the human Hdj1 (QIAN *et al.* 1996) is highly similar to the *E. coli* DnaJ J-domain (PELLACCHIA *et al.* 1996) and the two proteins share 54% amino acid identity in the J-domain (Figure 5D). We constructed a chimeric DnaJ expression plasmid, pGP18, which substituted the human Hdj1 J-domain coding sequence in place of the native *E. coli* DnaJ J-domain sequence. The hybrid DnaJ could fully subsititute for native DnaJ in each *in vivo* assay, indicating that the human J-domain could functionally substitute for the bacterial J-domain (in Figure 6, compare DnaJ and Hdj1). Next, we asked whether mutating any of the Hdj1 residues at the corresponding positions of the important DnaJ residues uncovered in our screen would result in similar inactivating phenotypes. To this end, alanine and glycine substitution mutants were engineered for Hdj1 Y24A, RR(25, 26)AA, K35G, N36G, and F45A and tested (see align-

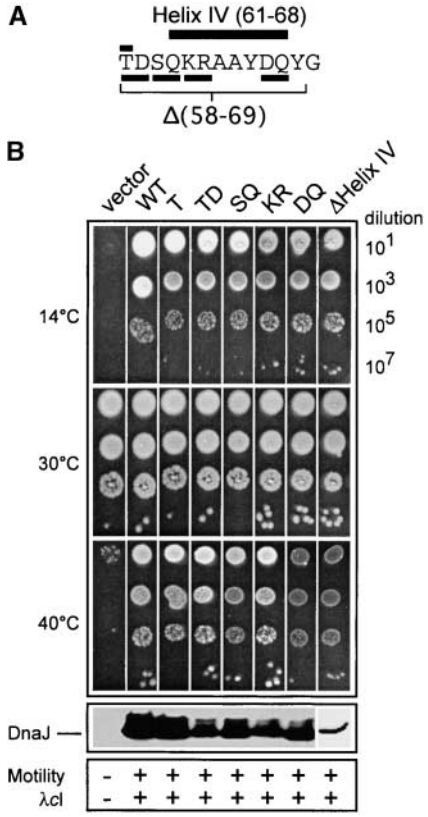

FIGURE 4.—Analysis of J-domain mutant phenotypes in helices III and IV loop and in helix IV. (A) The position of mutants is indicated by rectangles as single (above) or multiple mutants (below). (B) The functional complementation assays were performed as described in the legend to Figure 2A.

ment, Figure 5D). The numbering for the *hdj1* mutants uses the methionine start codon as 0, consistent with the PDB accession 1HDJ (QIAN *et al.* 1996). The results are shown in Figure 6. We observed that Y24A, RR(25,26)AA, and F45A abolished J-domain function for growth at both high and low temperatures. At higher arabinose concentrations, slow-growing colonies were observed for Y24A and a few colonies at 10^{-3} dilution were observed for F45A. The mutant Y24A weakly reduced λ plaque-forming efficiency, whereas RR(25,26)AA and F45A completely abolished λ plaque formation (efficiency of plating $<10^{-5}$) under all conditions tested. The Hdj1 mutant K35G behaved like its DnaJ counterpart, R36G, by showing marked effects on growth and λ plaque formation. In contrast and unlike the DnaJ N37G mutant, the Hdj1 N36G behaved like wild type in all assays (Figure 6).

Mapping essential residues on the J-domain structure: We mapped the critical residues Y25, K26, $_{33}$HPDRN$_{37}$, and F47 that we identified on the three-dimensional structure of the *E. coli* J-domain (Figure 5, A and B). Interestingly, these residues cluster in a small region on the same face of the J-domain. We also mapped the critical residues Y24, RR(25,26), K35, and F45 of Hdj1 on its J-domain three-dimensional structure (Figure 5C). As with DnaJ, these residues in Hdj1 also cluster together on the same spatial solvent-exposed face of the J-domain. Since most of other DnaJ mutants tested resulted in no detectable phenotype under any of our *in vivo* experimental conditions, we conclude that this compact region must encompass the totality, or major functional portion, of the J-domain interacting surface with DnaK.

DISCUSSION

In this study, we have used an exhaustive directed mutagenesis to identify residues in the *E. coli* DnaJ J-domain that are required for its cochaperone function with DnaK *in vivo*. Our extensive mutagenic screen has uncovered a new set of residues (Y25, K26, P34, R36, N37, and F47), in addition to those previously described, namely, *dnaJ*259 (H33Q) and *dnaJ*236 (D35N), that are important for J-domain function. Interestingly, all of these critical residues, located in helix II, helix III, and the helices II and III loop, project their side chains on the same solvent-exposed face of the J-domain. These same amino acids are highly conserved in the human Hdj1 J-domain and occupy a similar three-dimensional spatial arrangement (QIAN *et al.* 1996). Mutation of Hdj1 J-domain residues, in the context of a chimeric DnaJ-Hdj1 molecule, closely mirrors the corresponding mutation of DnaJ J-domain residues. This finding underscores the notion that the principal contact surface between a J-domain and the Hsp70 ATPase domain has been preserved through evolution and suggests that predictable inactivating mutations can be introduced in other J-domain proteins. We propose, therefore, that this region represents the principal contact surface interface between the J-domain and the Hsp70 ATPase domain.

It is surprising that we identified so few essential amino acid residues. Of the 48 residues mutated in the J-domain, only 8 resulted in a significant phenotype in our *in vivo* assays. These results, together with the fact that the *E. coli* DnaJ J-domain can be functionally replaced with a variety of distantly related J-domains—for instance, mammalian papovavirus T antigens (KELLEY and GEORGOPOULOS 1997; BERJANSKII *et al.* 2000), Mdj1 (DELOCHE *et al.* 1997), DjlA (GENEVAUX *et al.* 2001), Ydj1, and the bovine or *Torpedo* cysteine string protein (W. L. KELLEY, unpublished data)—would explain the apparent substitution plasticity observed with extensive multiple J-domain alignments (HENNESSY *et al.* 2000). Unlike *E. coli* DnaJ, SV40 T antigen tolerates only limited J-domain exchange from a related human virus JC, but does not function with J-domains from either *E. coli* DnaJ or Ydj1 (SULLIVAN *et al.* 2000).

Our *in vivo* genetic data are consistent with *in vitro* biochemical and biophysical studies that have attempted to map the J-domain interaction surface. Pep-

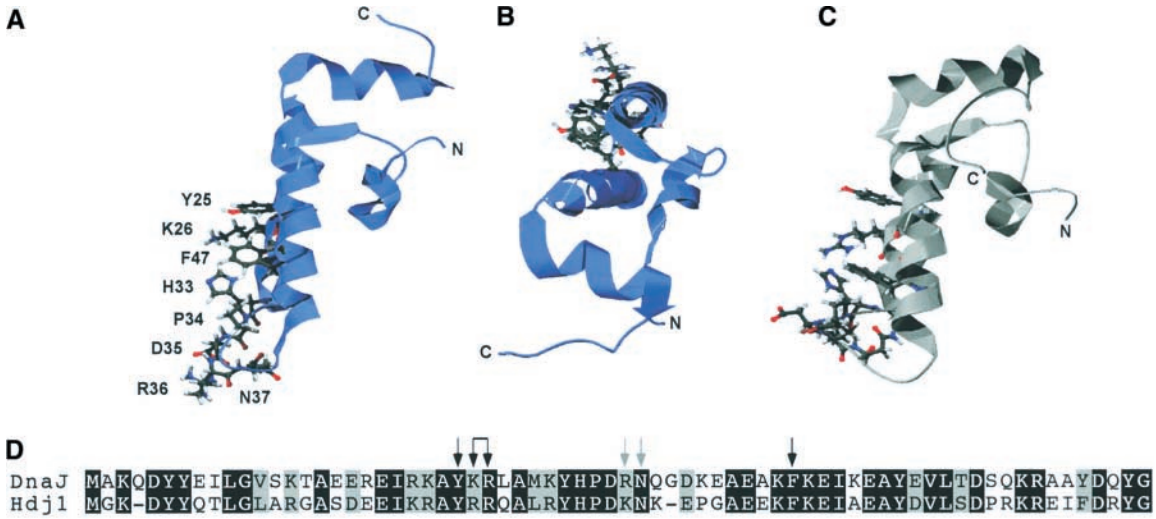

FIGURE 5.—Ribbon projection of *E. coli* DnaJ and human Hdj1 J-domains showing the tight surface clustering of important residues identified by mutational analysis. (A and B) Two views of the DnaJ J-domain together with marked essential side chain residues. B is a top projection down the *z*-axis of A, following a 90° clockwise rotation around the *z*-axis. (C) Human Hdj1 J-domain showing the location of essential residues in the same perspective as A. Figures were generated as described in the legend to Figure 2B. (D) Alignment of the *E. coli* J-domain and the human Hdj1 J-domain sequences. Identical residues are black, and conserved substitutions are gray. The location of the mutations is shown by arrows. Black indicates a change for alanine, and gray indicates a change for glycine.

tide competition studies using native *Saccharomyces cerevisiae* Ydj1p (Hsp40)-Ssa1p (Hsp70) interaction also predicted that the hinge region between αII and αIII, including HPD, mediated productive interaction with Hsp70 (CYR *et al.* 1992; TSAI and DOUGLAS 1996). Analysis of exclusively backbone amide proton chemical shifts by NMR perturbation mapping using *E. coli* DnaJ 2-75-DnaK titration led GREENE *et al.* (1998) to suggest that the minimal J-domain interaction surface could be composed of residues 2–35, including the HPD tripeptide. Out of the 17 residues identified by GREENE *et al.* (1998) that showed significant amide perturbation upon titration with DnaK(MgATP), 14 were mutated in our analysis, and only 4 (Y25, K26, H33, and D35) resulted in loss of function *in vivo*. Polypeptide backbone amide interactions, if important *in vivo*, may have been preserved in our mutants.

An electrostatic surface plot predicted that the DnaJ J-domain was highly asymmetric with respect to charge and that the positive face of helix II could provide an important recognition surface for the predominantly negative potential of the DnaK ATPase domain (PELLACCHIA *et al.* 1996; GREENE *et al.* 1998). Consistent with this prediction, ZIEGELHOFFER *et al.* (1995) noted that stimulation of the *S. cerevisiae* Ssa1p (Hsp70) ATPase by Ydj1p (Hsp40) was significantly affected by KCl titration (ZIEGELHOFFER *et al.* 1995). Our data support the prediction that the positive face of helix II is important for J-domain function and narrow it to residue K26 as the

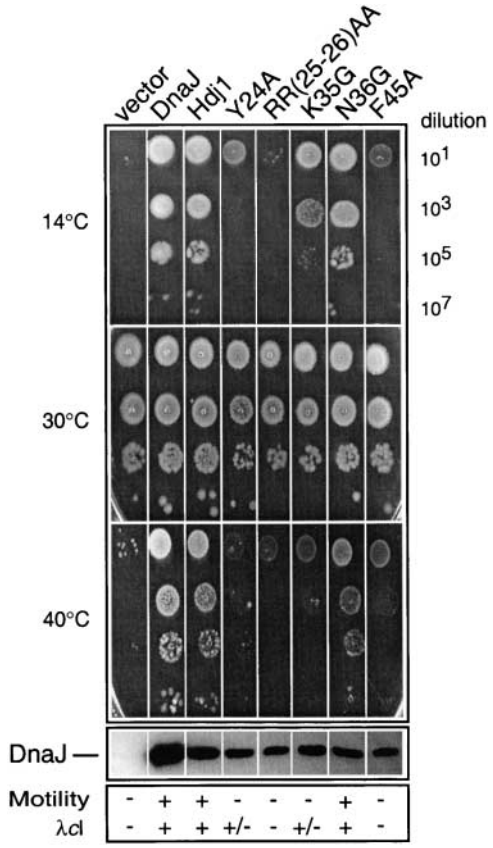

FIGURE 6.—Analysis of J-domain mutant phenotypes in the Hdj1 J-domain. The functional complementation assays were performed as described in the legend to Figure 2A.

only critical one. This finding is also in complete agreement with the prediction of Berjanskii *et al.* (2000) that the *b2* position of the helices II and III coiled coil of polyomavirus T antigen J-domain is the most essential positive charge position in helix II governing J-domain interactions with Hsp70 (Berjanskii *et al.* 2000). Indeed, polyomavirus T antigen J-domain can functionally substitute for DnaJ J-domain in our *in vivo* growth assays, despite lacking these conserved positive charge residues, except K35, which is equivalent to DnaJ K26 (Berjanskii *et al.* 2000).

The mechanistic role of the F47 residue is presently unclear. One possibility is that a bulky side chain projecting at this position may sterically constrain the limits of the helices II and III loop movement. This phenylalanine is highly conserved and positive charge residues flanking this residue have been proposed to play a role in mediating interaction with Hsp70 (Hennessy *et al.* 2000). In our study, mutation of the lysines flanking F47, and indeed nearly all surface-exposed residues of helix III, had no detectable effect *in vivo*. In contrast, in an attempt to understand Hsp40-Hsp70 partner specificity, Schlenstedt *et al.* (1995) showed that a single amino acid change, K42V, which is the positionally equivalent adjacent residue to DnaJ F47, could partially restore activity to an *S. cerevisiae* Sec63 chimera harboring a nonfunctional endoplasmic reticulum lumenal J-domain derived from cytoplasmic Sis1 (Schlenstedt *et al.* 1995).

Two *in vitro* studies suggest that the conserved $_{61}$QKRAA$_{65}$ motif of helix IV might contribute to binding to DnaK, although likely in the substrate cavity (Auger *et al.* 1996; Suh *et al.* 1998). Our work shows that single and double mutations along this region, as well as deletion of the entire αIV, had no significant phenotype. Although we cannot exclude that helix IV plays an as yet undetermined role in the biology of DnaJ, these results indicate that amino acid residues of αIV are not required for DnaJ to perform as DnaK cochaperone *in vivo*. Although polyomavirus and SV40 J-domains can replace DnaJ J-domain *in vivo* (Kelley and Georgopoulos 1997; Berjanskii *et al.* 2000), sequence comparison with the J-domain of either DnaJ or Hdj1 shows no significant conservation in the region of helix IV. In addition, the three-dimensional structures of the J-domains of polyomavirus and SV40 T antigens reveal a longer helix III and a long loop in place of helix IV, when compared to those of DnaJ and Hdj1. These results are in complete agreement with our findings.

Finally, the *E. coli* J-domain cannot by itself stimulate DnaK's ATPase and requires either an adjacent contiguous sequence, such as the Gly-Phe domain (G/F; Wall *et al.* 1994), or a costimulatory peptide/substrate that can interact with the DnaK substrate binding domain (Szabo *et al.* 1994; Karzai and McMacken 1996; Suh *et al.* 1998). A truncated DnaJ, containing residues 1–108 (DnaJ12), can perform some of the functions of wild-type DnaJ *in vivo* and can stimulate DnaK ATPase *in vitro*, suggesting that it contains minimal determinants for cochaperone function (Wall *et al.* 1994; Liberek *et al.* 1995). Using NMR methods, Huang *et al.* (1999) compared the structural changes in the J-domain that occur in the presence (DnaJ2-104) or absence (DnaJ2-78) of the adjacent G/F domain. Their results led to the proposal that the helices II and III loop and portions of helix II could adapt alternative conformations in the presence of G/F. In particular, a plot of the dihedral angles of residues in the helices II and III loop region revealed the possibility of a concerted hinge movement. Strikingly, the hinge region identified by Huang *et al.* (1999), $_{32}$YHPDR$_{36}$, and the contiguous $_{33}$HPDRN$_{37}$ pentapeptide harboring essential residues revealed in our study are nearly identical. The intriguing possibility is that this flexible loop/hinge region assumes alternative conformations that mediate reversible contact when paired with DnaK.

We thank Drs. Sam Landry and Maurizio Pellecchia for helpful discussions and Kyle Tanner for advice with PovRay. This work was supported by grant FN-31-065403.01 from the Swiss National Science Foundation and the Canton of Geneva.

LITERATURE CITED

Auger, I., J. M. Escola, J. P. Gorvel and J. Roudier, 1996 HLA-DR4 and HLA-DR10 motifs that carry susceptibility to rheumatoid arthritis bind 70-kD heat shock proteins. Nat. Med. **2:** 306–310.

Berjanskii, M. V., M. I. Riley, A. Xie, V. Semenchenko, W. R. Folk *et al.*, 2000 NMR structure of the N-terminal J domain of murine polyomavirus T antigens: implications for DnaJ-like domains and for mutations of T antigens. J. Biol. Chem. **275:** 36094–36103.

Bukau, B., and A. L. Horwich, 1998 The Hsp70 and Hsp60 chaperone machines. Cell **92:** 351–366.

Cyr, D. M., X. Lu and M. G. Douglas, 1992 Regulation of eukaryotic hsp70 function by a dnaJ homolog. J. Biol. Chem. **267:** 20927–20931.

Deloche, O., W. L. Kelley and C. Georgopoulos, 1997 Structure-function analyses of the Ssc1p, Mdj1p, and Mge1p *Saccharomyces cerevisiae* mitochondrial proteins in *Escherichia coli*. J. Bacteriol. **179:** 6066–6075.

Gassler, C. S., A. Buchberger, T. Laufen, M. P. Mayer, H. Schroder *et al.*, 1998 Mutations in the DnaK chaperone affecting interaction with the DnaJ cochaperone Proc. Natl. Acad. Sci. USA **95:** 15229–15234.

Gassler, C. S., T. Wiederkehr, D. Brehmer, B. Bukau and M. P. Mayer, 2001 Bag-1M accelerates nucleotide release for human Hsc70 and Hsp70 and can act concentration-dependent as positive and negative cofactor. J. Biol. Chem. **276:** 32538–32544.

Genevaux, P., A. Wawrzynow, M. Zylicz, C. Georgopoulos and W. L. Kelley, 2001 DjlA is a third DnaK co-chaperone of *Escherichia coli*, and DjlA-mediated induction of colanic acid capsule requires DjlA-DnaK interaction. J. Biol. Chem. **276:** 7906–7912.

Greene, M. K., K. Maskos and S. J. Landry, 1998 Role of the J-domain in the cooperation of Hsp40 with Hsp70. Proc. Natl. Acad. Sci. USA **95:** 6108–6113.

Hartl, F. U., 1996 Molecular chaperones in cellular protein folding. Nature **381:** 571–580.

Hennessy, F., M. E. Cheetham, H. W. Dirr and G. L. Blatch, 2000 Analysis of the levels of conservation of the J domain among the various types of DnaJ-like proteins. Cell Stress Chaperones **5:** 347–358.

Higuchi, R., B. Krummel and R. K. Saiki, 1988 A general method of *in vitro* preparation and specific mutagenesis of DNA fragments: study of protein and DNA interactions. Nucleic Acids Res. **16:** 7351–7367.

Hill, R. B., J. M. Flanagan and J. H. Prestegard, 1995 ^{1}H and

^{15}N magnetic resonance assignments, secondary structure, and tertiary fold of *Escherichia coli* DnaJ (1-78). Biochemistry **34:** 5587–5596.

Huang, K., R. Ghose, J. M. Flanagan and J. H. Prestegard, 1999 Backbone dynamics of the N-terminal domain in *E. coli* DnaJ determined by ^{15}N- and ^{13}CO-relaxation measurements. Biochemistry **38:** 10567–10577.

Karzai, A. W., and R. McMacken, 1996 A bipartite signaling mechanism involved in DnaJ-mediated activation of the *Escherichia coli* DnaK protein. J. Biol. Chem. **271:** 11236–11246.

Kelley, W. L., 1998 The J-domain family and the recruitment of chaperone power. Trends Biochem. Sci. **23:** 222–227.

Kelley, W. L., and C. Georgopoulos, 1997 The T/t common exon of simian virus 40, JC, and BK polyomavirus T antigens can functionally replace the J-domain of the *Escherichia coli* DnaJ molecular chaperone. Proc. Natl. Acad. Sci. USA **94:** 3679–3684.

Kim, H.-Y., B.-Y. Ahn and Y. Cho, 2001 Structural basis for the inactivation of retinoblastoma tumor suppressor by SV40 large T antigen. EMBO J. **20:** 295–304.

Kunkel, T. A., J. D. Roberts and R. A. Zakour, 1987 Rapid and efficient site-specific mutagenesis without phenotypic selection. Methods Enzymol. **154:** 367–383.

Liberek, K., J. Marszalek, D. Ang, C. Georgopoulos and M. Zylicz, 1991 *Escherichia coli* DnaJ and GrpE heat shock proteins jointly stimulate ATPase activity of DnaK. Proc. Natl. Acad. Sci. USA **88:** 2874–2878.

Liberek, K., D. Wall and C. Georgopoulos, 1995 The DnaJ chaperone catalytically activates the DnaK chaperone to specifically bind the σ^{32} heat shock transcriptional regulator. Proc. Natl. Acad. Sci. USA **92:** 6224–6228.

Lyman, S. K., and R. Schekman, 1997 Binding of secretory precursor polypeptides to a translocon subcomplex is regulated by BiP. Cell **88:** 85–96.

Misselwitz, B., O. Staeck and T. A. Rapoport, 1998 J proteins catalytically activate Hsp70 molecules to trap a wide range of peptide sequences. Mol. Cell **2:** 593–603.

Peden, K. W., and J. M. Pipas, 1992 Simian virus 40 mutants with amino-acid substitutions near the amino terminus of large T antigen. Virus Genes **6:** 107–118.

Pellacchia, M., T. Szyperski, D. Wall, C. Georgopoulos and K. Wüthrich, 1996 NMR structure of the J-domain and the Gly/Phe-rich region of the *Escherichia coli* DnaJ chaperone. J. Mol. Biol. **260:** 236–250.

Qian, Y. Q., D. Patel, F.-U. Hartl and D. J. McColl, 1996 Nuclear magnetic resonance solution structure of the human Hsp40 (HDJ-1) J-domain. J. Mol. Biol. **260:** 224–235.

Raabe, T., and J. L. Manley, 1991 A human homologue of the *Escherichia coli* DnaJ heat shock protein. Nucleic Acids Res. **19:** 6645.

Schlenstedt, G., S. Harris, B. Risse, R. Lill and P. A. Silver, 1995 A yeast DnaJ homologue, Scj1p, can function in the endoplasmic reticulum with BiP/Kar2p via a conserved domain that specifies interactions with Hsp70's. J. Cell Biol. **129:** 979–988.

Shi, W., Y. Zhou, J. Wild, J. Adler and C. A. Gross, 1992 DnaK, DnaJ, and GrpE are required for flagellum synthesis in *Escherichia coli*. J. Bacteriol. **174:** 6256–6263.

Suh, W. C., W. F. Burkholder, C. Z. Lu, X. Zhao, M. E. Gottesman *et al.*, 1998 Interaction of the Hsp70 molecular chaperone, DnaK, with its cochaperone DnaJ. Proc. Natl. Acad. Sci. USA **95:** 15223–15228.

Sullivan, C. S., J. D. Tremblay, S. W. Fewell, J. A. Lewis, J. L. Brodsky *et al.*, 2000 Species-specific elements in the large T-antigen J domain are required for cellular transformation and DNA replication by simian virus 40. Mol. Cell. Biol. **20:** 5749–5757.

Szabo, A., T. Langer, H. Schröder, J. Flanagan, B. Bukau *et al.*, 1994 The ATP hydrolysis-dependent reaction cycle of the *Escherichia coli* Hsp70 system-DnaK, DnaJ, and GrpE. Proc. Natl. Acad. Sci. USA **91:** 10345–10349.

Szyperski, T., M. Pellacchia, D. Wall, C. Georgopoulos and K. Wüthrich, 1994 NMR structure determination of the *Escherichia coli* DnaJ molecular chaperone: secondary structure and backbone fold of the N-terminal region (residues 2–108), containing the highly conserved J-domain. Proc. Natl. Acad. Sci. USA **91:** 11343–11347.

Tsai, J., and M. G. Douglas, 1996 A conserved HPD sequence of the J-domain is necessary for YDJ1 stimulation of hsp70 ATPase activity at a site distinct from substrate binding. J. Biol. Chem. **271:** 9347–9354.

Ueguchi, C., T. Shiozawa, M. Kakeda, H. Yamada and T. Mizuno, 1995 A study of the double mutation of *dnaJ* and *cbpA*, whose gene products function as molecular chaperones in *Escherichia coli*. J. Bacteriol. **177:** 3894–3896.

Wall, D., M. Zylicz and C. Georgopoulos, 1994 The NH_2-terminal 108 amino acids of the *Escherichia coli* DnaJ protein stimulate the ATPase activity of DnaK and are sufficient for λ replication. J. Biol. Chem. **269:** 5446–5451.

Wild, J., E. Altman, T. Yura and C. A. Gross, 1992 DnaK and DnaJ heat shock proteins participate in protein export in *Escherichia coli*. Genes Dev. **6:** 1165–1172.

Ziegelhoffer, T., P. Lopez-Buesa and E. A. Craig, 1995 The dissociation of ATP from hsp70 of *Saccharomyces cerevisiae* is stimulated by both Ydj1p and peptide substrates. J. Biol. Chem. **270:** 10412–10419.

Communicating editor: A. L. Sonenshein